RESEARCH ARTICLE

Macromolecular Chemistry and Physics
www.mcp-journal.de

Surface-Attached Polymer Networks Made from Cationic Poly(diitaconates): Synthesis, Surface Characterization, and Bioactivity

*Alexandra Schneider-Chaabane, David Boschert, Sibylle Rau, Diana Lorena Guevara Solarte, Vera Bleicher, Ali Al-Ahmad, and Karen Lienkamp**

Facially amphiphilic polymers carrying cationic and hydrophobic groups on the same repeat unit have shown promising antimicrobial activity and biocompatibility, yet they are prone to suffer from protein adhesion which may induce biofilm formation. To overcome this problem, poly(diitaconate)-based copolymers with cationic/hydrophobic and protein-repellent/charge-neutral repeat units are synthesized. The bioactivity profile of surface-attached polymer networks made from these copolymers depends on the ratio of the cationic and charge-neutral repeat units. In all cases, the protein adhesion is substantially reduced compared to purely cationic polymers. At a 50:50 ratio, the polymer coatings are partially protein-repellent and antimicrobial, yet slightly cell toxic. At an intermediate composition of 30:70, they are still antimicrobial and the cell compatibility is substantially improved. The long-term stability of these materials still has to be determined to judge their suitability for medical applications.

1. Introduction

Antimicrobial agents and materials are direly needed to prevent the spreading of resistant bacteria in hospitals and other care facilities. In this context, polycationic materials and surface coatings have received considerable attention. They can be derived either from synthetic polycations[1–5] or from natural polymers like chitin,[6] and are typically either poly(ammonium), poly(phosphonium), or poly(*N*-alkylvinylpyridine) salts.[7–16] The common feature of these contact-active antimicrobial polymer surfaces is their hydrophobicity and charge density.[17] They attract the negatively charged cell envelopes of bacteria and bind them to the surface, so that the bacterial cell membrane integrity is compromised, and bacterial proliferation is suppressed. The exact mechanism for this process is not yet understood in detail,[17,18] although it is clear that the effect is local, i.e., contact-related, and probably mainly a physical one.[17]

To obtain polycationic surfaces with low cell toxicity, their hydrophobicity must be properly balanced, as has been shown, e.g., for a series of poly(oxanorbornene)-based polymer coatings.[19] These have been inspired by synthetic mimics of antimicrobial peptides (SMAMPs).[20] SMAMPs are low molar mass, facially amphiphilic molecules with hydrophobic and cationic groups on opposite sides of the molecule, and mimic the structure and mode of activity of antimicrobial peptides (AMPs).[21,22] Like AMPs, SMAMPs target the bacterial cell envelope by an unspecific, potentially multitarget mechanism, which ultimately leads to damage of the cell membrane, leakage of cytosol, and cell death.[20–36] In contrast to antibiotics, AMPs and SMAMPs are much less prone to develop bacterial resistance.[36–42] The groups of polymer-based SMAMPs that have been investigated in most detail are poly(oxanorbornene)-based,[20,27,29–31,43,44] poly(methacrylate)-based,[24,33,34,42,45–53] or nylon-3 based.[21,22,54] At high molar mass, SMAMPs can be turned into surface-attached polymer coatings which are highly active against bacteria, yet do not compromise the viability of mammalian cells due to their precisely balanced amphiphilicity.[19]

While polycationic surfaces show promising antimicrobial activity and in the case of many SMAMP-coated surfaces also good biocompatibility, one general disadvantage of polycationic

A. Schneider-Chaabane, D. Boschert, V. Bleicher, K. Lienkamp
Bioactive Polymer Synthesis and Surface Engineering Group
Department of Microsystems Engineering (IMTEK) and Freiburg Center for Interactive Materials and Bioinspired Technologies (FIT)
University of Freiburg
Georges-Köhler-Allee 105, 79110 Freiburg, Germany
E-mail: karen.lienkamp@uni-saarland.de
S. Rau, D. L. G. Solarte, A. Al-Ahmad
Department of Operative Dentistry and Periodontology
Medical Center of the University of Freiburg
Faculty of Medicine
University of Freiburg
Hugstetter Str. 55, 79106 Freiburg, Germany
K. Lienkamp
Department of Materials Science
Saarland University Campus
66123 Saarbrücken, Germany

The ORCID identification number(s) for the author(s) of this article can be found under https://doi.org/10.1002/macp.202200323

DOI: 10.1002/macp.202200323

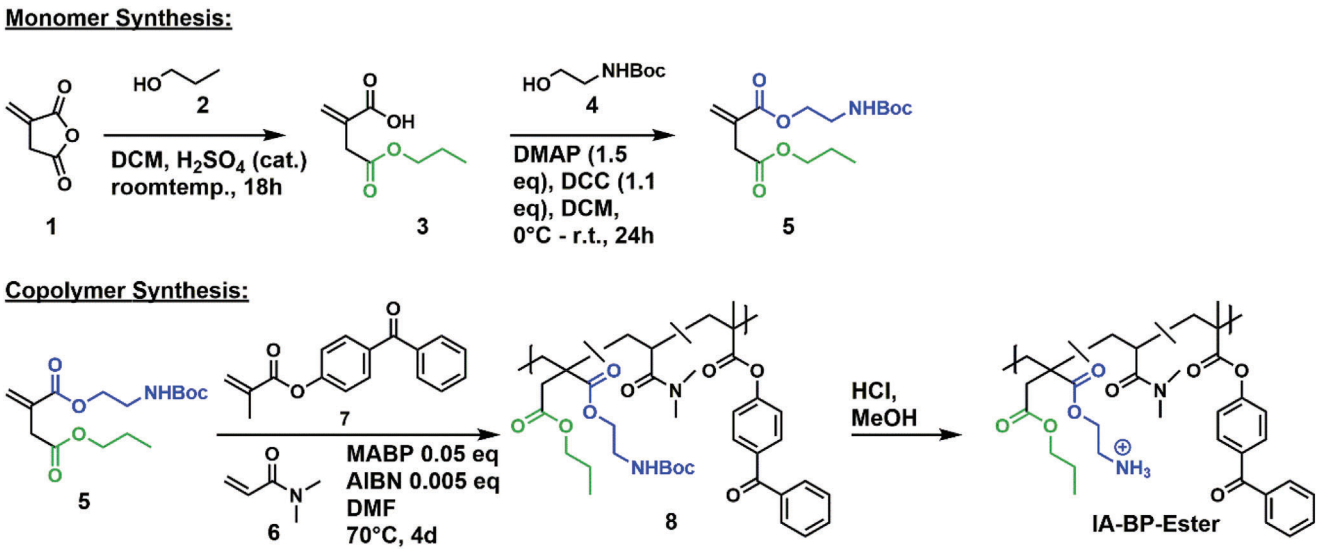

Figure 1. Monomer and copolymer synthesis. The functional monomer **5** was obtained via two esterification steps from itaconic anhydride **1**. It was copolymerized in different ratios with *N*,*N*-dimethylacrylamide (DMAA) **6** and the cross-linker monomer MABP **7** to yield the target polymer **8** in its *N*-Boc protected form.

surface coatings is their propensity to not only capture and kill bacteria, but to also attract negatively charged biomolecules like proteins and lipids, or the debris of dead bacteria. This leads to surface contamination and biofilm formation.[55,56] To reduce this problem, one strategy is to decrease the number of charged repeat units of the cationic surface to the bare minimum for sufficient activity, e.g., by "diluting" them with charge-neutral repeat units. Following this strategy, the aim of the present study was to synthesize antimicrobial copolymers with varying amounts of cationic and charge-neutral, protein-repellent repeat units, and to use these polymers as coatings for various substrates. The ratio of active and diluting repeat units was varied to optimize the antimicrobial activity and protein repellency of the materials.

As synthetic platform for the antimicrobial component, poly(diitaconates) were chosen. They can be derived from itaconic acid, a building block based on renewable resources. The here presented poly(diitaconates) carry two functional groups per repeat unit, so that their facial amphiphilicity can be precisely tuned. Unlike previously reported facially amphiphilic poly(oxanorbornenes), poly(diitaconates) can be synthesized without the use of expensive or potentially toxic metal catalysts. Poly(diitaconate)-based SMAMPs have shown considerable antimicrobial activity, yet sufficient cell compatibility as low molar mass polymers in solution.[57,58] Diitaconates can be copolymerized with acrylic monomers by controlled or free radical polymerization.[57,58] From the many charge-neutral, hydrophilic and commercially available comonomers to choose from, *N*,*N*-dimethylacrylamide (DMAA) was selected as a diluting comonomer due to the known cell compatibility and strong protein repellency of the poly(*N*,*N*-dimethylacrylamide) (PDMAA) polymer.[59] Methacryloxy benzophenone (MABP) was used as an additional monomer as it is an efficient intramolecular cross-linker to form polymer networks.[60] Combined with surface-attached benzophenone anchor groups,[61] MABP-containing polymers can be cross-linked and surface-attached in a single step, as pioneered by Rühe and co-workers.[62]

2. Results and Discussion

2.1. Study Design

In order to obtain antimicrobial polymer surfaces with a reduced propensity to be contaminated by negatively charged biomolecules, copolymers of cationic diitaconate (as active repeat units), charge-neutral *N*,*N*-dimethylacrylamide (DMAA, as dilutant repeat units), and benzophenone-substituted methacrylate repeat units (MABP, as built-in UV cross-linkers) were synthesized (**Figure 1**). These polymers could be spin-coated onto pre-functionalized substrates and would form surface-attached polymer coatings when UV irradiated.

The structure of the target copolymer (named **IA-BP-Ester**) is shown in Figure 1. Each diitaconate repeat unit carries one hydrophilic ethylammonium group and one hydrophobic propyl group as substituents. Copolymers with about 10%, 30%, and 50% of diitaconate repeat units (in their *N*-tert-butylcarbamate (*N*-Boc) protected form), about 5% MABP repeat units, and about 90%, 70%, and 50% DMAA repeat units were synthesized. Thus, while the amount of MABP cross-linker units was kept constant, the ratio of the cationic and the neutral repeat units, which influenced the bioactivity profile of the polymer, was varied. Three copolymers with different repeat unit ratios (named 50:50:5, 30:70:5, and 10:90:5 in the following according to their diitaconate: DMAA: MABP content), were obtained.

2.2. Monomer and Polymer Synthesis

The synthesis of the target copolymers is illustrated in Figure 1. In short, itaconic acid anhydride (**1**) was ring-opened with

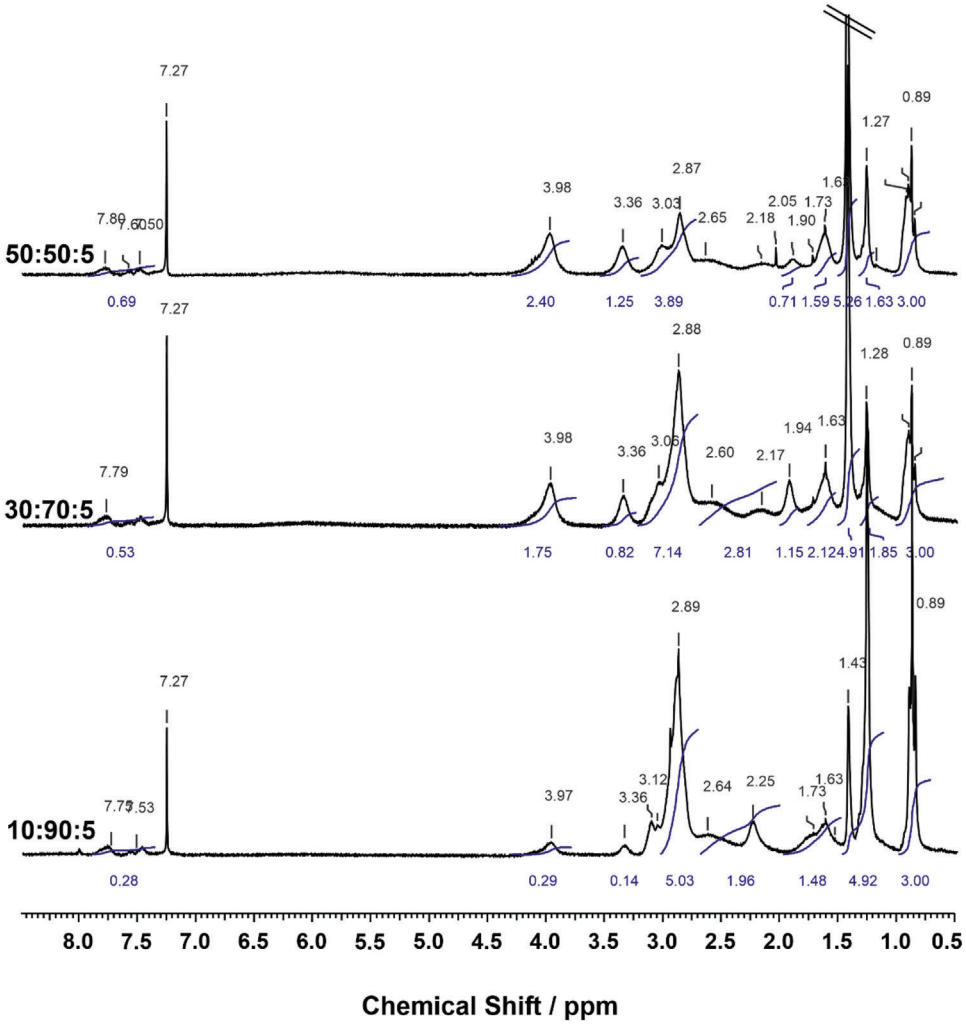

Figure 2. ^{1}H-NMR spectra of the protected **IA-BP-Ester** copolymers with different repeat unit ratios (in $CDCl_3$). The peak at 1.43 ppm is assigned to the Boc-protective group, the signals from 2.75 – 3.05 to the methyl groups of DMAA. The signals at 3.36 and 3.98 are assigned to the methylene groups of the ester group of the diitaconate moiety, and the signal between 7.6 – 7.9 ppm to the MABP aryl groups. Traces of ethanol are found at 1.25 and 3.72 ppm, respectively.

1-propanol (**2**) to give the intermediate **3**. This product was esterified with 2-*N*-Boc-aminoethanol **4** using Steglich conditions to yield the 1-(2'-*N*-Boc-aminoethyl) 4-propyl diitaconate monomer **5**, as previously reported.[57] ^{1}H-NMR spectra of intermediate **3** and monomer **5** are given in Figure S1 (Supporting Information). The target monomer was copolymerized with DMAA (**6**) and MABP (**7**) using free-radical polymerization in *N,N*-dimethyl formamide (DMF), with azoisobutyronitrile (AIBN) as initiator to yield the *N*-Boc protected copolymer **8**. The different copolymers were purified by precipitation and were characterized via ^{1}H NMR spectroscopy, gel permeation chromatography (GPC), and differential scanning calorimetry (DSC). The ^{1}H-NMR spectra of these polymers are shown in **Figure 2**. Signals of the *N*-Boc protective group, the methylene groups between the two oxygen atoms, the DMAA methyl groups, and the aryl groups of the benzophenone ring could be assigned, which confirmed that all the desired functional groups were present. By integration of their characteristic peaks in the ^{1}H-NMR spectra, the ratio of these three repeat units was determined, as summarized in **Table 1**. In general, the targeted repeat unit ratios (50:50:5, 30:70:5, and 10:90:5) were relatively closed to the ones obtained in the experiments, indicating that none of the repeat units was preferentially

Table 1. Repeat unit content and characterization data of the **IA-BP-Ester** copolymers. The repeat unit ratio was determined by ^{1}H NMR spectroscopy, the number average molar mass (M_n), the weight average molar mass (M_w) and the polydispersity indices (PDI) were obtained by gel permeation chromatography (GPC).

IA-BP-Ester	Repeat unit ratios [mol%]			T_g [°C]	M_n [g mol^{-1}]	M_w [g mol^{-1}]	PDI
	IA-Ester	DMAA	MABP				
50:50:5	46	52	3	63.5	26800	62800	2.3
30:70:5	26	71	4	58.6	46100	410000	8.9
10:90:5	8	89	3	59.0	53300	520000	9.8

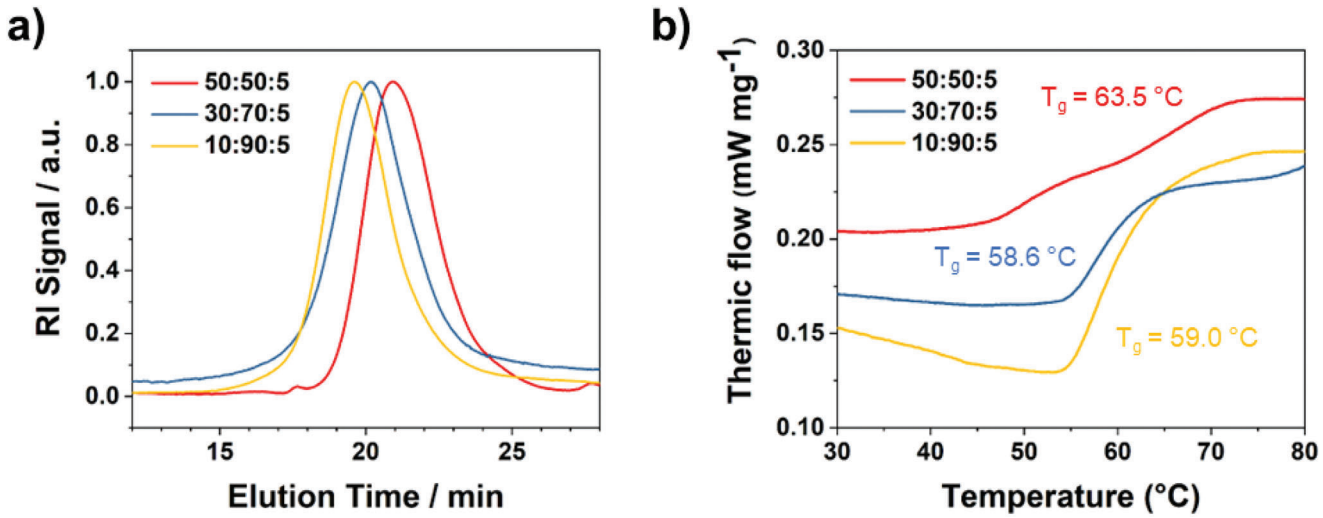

Figure 3. a) Gel permeation chromatography elugrams (in chloroform, flow rate 1 mL min^{-1}, SDV columns), and b) DSC curves of of the protected copolymers **8** with different repeat unit ratios.

incorporated into the polymer. This confirmed previous results for low molar mass diitaconate copolymers.[57,58] In these studies, we had determined the copolymerization parameters for the diitaconate-DMAA system and found no significant preferential incorporation of either monomer into the polymer in free radical polymerization.

The corresponding GPC elugrams are shown in **Figure 3**a and indicate that a monomodal molar mass distribution function was obtained. As listed in Table 1, the obtained number average molar masses M_n ranged from 26 800 to 53 300 g mol^{-1}, with polydispersity indices (PDI) from 2.3 to 9.8. This is a rather large polydispersity, even for free radical polymerization, and is attributed to chain transfer to solvent, which is frequently encountered when polymerizing itaconates, as reported previously.[57,58] This leads to a rather large fraction of low molar mass species, which is observed as persistent tailing at the low molar mass flank of the GPC elugrams.

While a high polydispersity would be a problem for fine-tuning of the antimicrobial activity of low molar mass polymers in solution (because it is molar mass-dependent), the PDI is irrelevant for surface-attached polymer networks. After cross-linking, each network is one chemical entity with infinite molar mass, and its bioactivity depends more on surface coverage and chain mobility than on the molar mass of the polymers used. Importantly, the molar mass of each copolymer was high enough to prepare polymer solutions with a sufficiently high viscosity for spin-coating.

The glass transition temperatures (T_g) of the protected copolymers were 63.5 °C (50:50:5), 58.4 °C (30:70:5), and 59.0 °C (10:90:5), as determined by differential scanning calorimetry (Figure 3b). As expected, there was only one T_g for the copolymers with a ratio of 30:70:5 and 10:90:5, indicating a statistical distribution of the repeat units in the polymer. These data are in agreement with T_g measurements performed recently with low-molar mass diitaconate ester-co-DMAA-copolymers, which had a T_g of 65.4 °C.[63] However, it appears that there is a second T_g of around 50 °C for the sample with the 50:50:5 ratio. This second T_g does not correspond to the T_g of PDMAA homopolymers (which is around 106 °C) and does not appear in the other copolymer samples with the lower diitaconate content. The raw data of this measurement is shown in Figure S3 (Supporting Information), together with the first derivative of the heat flow curve. Because these transitions are relatively broad and shallow in the heat flow curve, the corresponding two peaks of the first derivative are also indistinct and have a low signal to noise ratio. Yet they confirm the second T_g. It is possible that there are two kinds of blocky sequences in the 50:50:5 copolymer, one DMAA-rich, the other diitaconate-rich, and that these have slightly different T_g values. This has to be confirmed by further research, which is beyond the scope of this work, and therefore this data should not be over-interpreted.

To obtain the **IA-BP-Esters**, the *N*-Boc protective groups of copolymers **8** were cleaved with hydrochloric acid (HCl). This was either done before coating, or after coating on the substrate as indicated below. The ^{1}H-NMR spectra of the solution-deprotected **IA-BP-Esters** are shown in Figure S2 (Supporting Information) and indicate that the *N*-Boc protective group previously observed at 1.44 ppm was successfully removed.

2.3. Fabrication of Surface Coatings

2.3.1. Surface Pre-Functionalization

To covalently attach the target copolymers onto different substrates, the substrates had to be pre-functionalized with anchor groups containing benzophenone. As reported previously, this was achieved by reacting silicon wafers or glass substrates with 4-(3-triethoxysilyl) propylbenzophenone (**3EBP**, **Figure 4**a); the gold-coated glass substrates needed for the protein adhesion studies were coated with lipoic acid that was functionalized with benzophenone (**LS-BP**, Figure 4a).[19] When these surfaces pre-functionalized with benzophenone are coated with a polymer and UV-irradiated, covalent bonds form between nearby alkyl chains

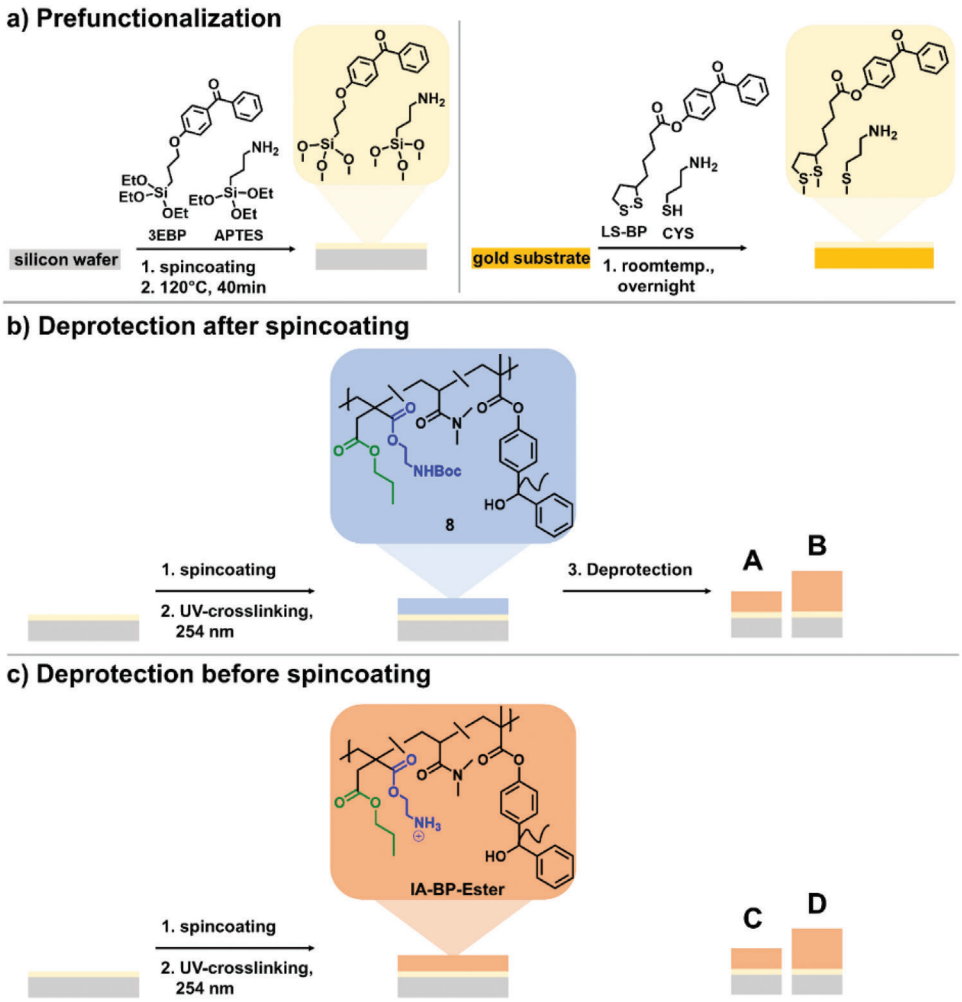

Figure 4. a) Pre-functionalization of the substrates. Left: Silicon wafers were functionalized with a 1:1 mixture of 4-(3-triethoxysilyl) propylbenzophenone (**3EBP**) and (3-aminopropyl) triethoxysilane (**APTES**). Right: Gold substrates were reacted with a 1:1 mixture of **LS-BP** and **CYS**. b) Coating processes **A** and **B**: The different copolymers **8** were spin-coated onto the pre-functionalized substrates and deprotected on the surface. Coating **A** is a single layer, coating **B** is a bilayer; c) Coating processes **C** and **D**: The different **IA-BP-Ester** copolymers were coated onto the pre-functionalized wafers. Coating **C** is a single layer, coating **D** is a bilayer.

and the surface-attached benzophenone groups through a C,H insertion reaction.[62]

For bioactivity studies, it is crucial that homogeneous, almost defect-free surface coatings are obtained. As surfaces densely functionalized with benzophenone groups become hydrophobic, coating them with the hydrophilic diitaconate copolymers would lead to dewetting defects. To prevent this, the silicon and glass substrates used in this work were pre-treated with a mixture of **3EBP** and the more hydrophilic 3-aminopropyl triethoxysilane (**APTES**), and the gold substrates with mixture of **LS-BP** and the amino acid derivative cysteamine (**CYS**). We reported this general procedure before,[64] yet it is important to note that the ratio of the hydrophobic and the hydrophilic surface functionalization reagent has to be optimized for each polymer system to obtain an optimized surface coating morphology. We also tested mixtures of **APTES** and triethoxypropyl silane instead of **3EBP** for pre-functionalization because triethoxypropyl silane is less hydrophobic than **3EBP**. When substrates pre-functionalized with **APTES** and triethoxypropyl silane and coated with the target copolymers are UV irradiated, covalent bonds can form by C,H-insertion reactions between the propyl group of the surface and the benzophenone group of the polymer, thus ensuring surface attachment. The results of the pre-functionalization studies are shown in Figures S4 and S5, Table S3 (Supporting Information). As can be seen from this data, coatings with the least number of defects and the lowest roughness were obtained when using **3-EBP** and **APTES** at a ratio of 1:1. This prefunctionalization recipe was therefore used in the following.

2.4. Fabrication of Surface-Attached Polymer Networks

To obtain surface-attached polymer networks with optimized layer homogeneity, four different coating methods were tested (**A–D**, as illustrated in Figure 4). For coating type **A**, the surfaces were spin-coated with the protected copolymer **8** and

UV-irradiated at 254 nm with an energy of 3 J. They were then deprotected with HCl in dioxane to obtain the deprotected **IA-BP-Ester** surfaces and washed with ethanol and acetic acid to remove unbound polymer chains. To obtain coating type **B**, the surfaces were spin-coated with a solution of copolymer **8** and UV-irradiated in the same manner. Then, a second coating was applied and UV irradiated using the same conditions, followed by the same deprotection and washing steps as described for **A**. For coating types **C** and **D**, the surfaces were coated with a solution of the deprotected **IA-BP-Ester** instead of the protected copolymer. Otherwise, the coating and washing steps were analogous to methods **A** and **B**, respectively, yielding a single layer and a double layer coating of **IA-BP-Ester**.

Overall, the surface characterization data described below showed that the protected copolymer **8** yielded more homogeneous coatings compared to coatings obtained from the deprotected **IA-BP-Ester**, and that two coatings gave a better surface coverage than one coating.

2.5. Chemical and Physical Characterization

The different coating types **A**–**D** thus obtained for each of the **IA-BP-Ester** copolymers have been studied by FTIR spectroscopy to confirm the success of the coating process and the deprotection step, as summarized in Figure S6 (Supporting Information). The spectra in this figure confirm that the expected functional groups are present. As all spectra were normalized to the same background, they also semi-quantitatively show by their peak intensities the expected changes in peak intensities for the **IA-BP-Ester** with different repeat unit ratios. The layer thickness of each coating was determined by ellipsometry, as summarized in **Table 2**. In each case, the layer thickness before and after the washing step was determined. The data indicates that the thickness loss after washing was minimal. All samples had a gel content (= ratio of thickness before washing and after washing, multiplied by 100) of at least 92%. The thickness loss of samples that were deprotected on the surface (coating types **A** and **B**) was more substantial than for coatings made from already deprotected **IA-BP-Ester** copolymers, which can be explained by the extraction of polymer chains that only had cross-links to the alkyl chains of the *N*-Boc protective groups. Still, the thickness of the coatings prepared by on-surface deprotection was higher than that of the samples that were directly obtained from the deprotected **IA-BP-Ester** copolymers. The static, advancing and receding contact angles overall decreased from 50:50:5 to 10:90:5, i.e., with higher DMAA content of the polymer. This is in line with expectations, as the DMAA-based repeat units are more hydrophilic than the diitaconate repeat units. The coatings **A**–**D** made from the same copolymer, but with different coating techniques, showed deviations as much as ± 20 ° in some of the static and advancing contact angles, e.g., between 50:50:5 **B** and 50:50:5 **C**, or between 30:70:5 **B** and 30:70:5 **C**. This is in line with our previous experience that contact angle data of highly hydrophilic coatings (which swell during the measurement) are difficult to measure reproducibly as the measurements are not done in equilibrium and should in general not be over-interpreted. In this case, the coatings **A**–**D** additionally differed in their preparation conditions, which can affect both the coating roughness and the internal organization of the polymer chains, and thus contributes to further numerical deviation. Yet as a data ensemble, the measurements show the expected trend.

The surface morphology and roughness of the four coating types of each polymer were studied by atomic force microscopy (AFM, **Figure 5** and **Table 2**). In all cases, the double layer coatings were smoother than their single layer counterparts. Additionally, it was observed that the surface roughness significantly increased with increasing DMAA content due to defect formation.

For example, in the AFM height images of the single layer coatings 10:90:5 **A** and 10:90:5 **C**, pronounced dewetting defects can be seen. These are closed to a certain extent by the double layer structure of 10:90:5 **B** and 10:90:5 **D**, yet an overall increased roughness remains in these materials compared to the samples with lower DMAA content. In general, the surface-attached polymer networks **A** and **B** obtained by spin-coating polymers **8** from organic solution had a lower roughness and a better homogeneity than the coatings obtained from an aqueous solution of the deprotected **IA-BP-Ester** copolymers. Thus, procedure **B** gave the best results in terms of homogeneity for these materials.

The pH-dependent surface zeta potential measured for the different **IA-BP-Ester** copolymer networks (50:50:5, 30:70:5, 10:90:5, all of coating type **B**) is shown in **Figure 6**, and the results are summarized in **Table 3**. The data show that the zeta potential of these coatings at physiological pH (located at the cross-points of the titration curves with the vertical line at pH 7.4 in Figure 6) is overall positive, as would be expected for surfaces coated with cationic polymers. The curves of 50:50:5 and 30:70:5 are very similar, except for a marked shift of the isoelectric points, which are given by the cross-points of the titration curves with the horizontal line in Figure 6. In contrast, the zeta potential of the polymer with only 10% diitaconate content is not only significantly lower throughout, but the isoelectric point is even further shifted to lower pH. Thus, there is a trend to lower isoelectric points with decreasing diitaconate content, i.e., increasing hydrophilicity of the sample. Further, from the zeta potential data, it is expected that the propensity of the networks to capture negatively charged biomolecules decreases in the order 50:50:5 > 30:70:5 > 10:90:5, just like the zeta potential under physiological conditions.

2.6. Protein Adhesion

As a model for negatively charged biomolecules, the adhesion of the negatively charged protein fibrinogen on the different coatings was studied by surface plasmon resonance spectroscopy at pH 7.4 and 37 °C (pseudo-physiological conditions, **Figure 7**). As this method is extremely sensitive to substrate imperfections, only the **B** type coatings were investigated. For the first sample set, two types of measurements were performed. First, full angular scans (reflectivity vs angle) were measured on the dry sample before contact with the protein solution. Next, in a kinetics experiment (reflectivity measurement at constant angle vs time), a solution of fibrinogen in buffer was flown over the substrates, followed by washing with pure buffer. This allowed to monitor the protein adhesion process in situ. In the last step, the surface was washed with deionized water and dried, and another full angular reflectivity scan was taken. The data for the kinetics experiment for all type **B IA-BP-Ester** coatings is shown in Figure 7a;

Table 2. Physical characterization of silicon substrates coated with the three different **IA-BP-Ester** copolymers using four different coating methods (**A**–**D**). c = concentration of the polymer solution used for spin-coating. The coating thickness was measured by ellipsometry, the roughness was determined by atomic force microscopy.

IA-BP-Ester	c [mg mL^{-1}]	Coating method	Thickness [nm] before extraction	Thickness [nm] after extraction	Thickness [nm] after deprotection	Gel content [%]	Contact angle [°] static, adv., rec.	Rough-ness [nm]
50:50:5	20	A	169 ± 1	160 ± 0	137 ± 0	95	64 ± 1 69 ± 2 36 ± 4	0.92
		B	311 ± 1	299 ± 1	252 ± 1	96	68 ± 3 68 ± 2 41 ± 4	0.52
		C	137 ± 0	133 ± 1	-	97	69 ± 0 87 ± 0 46 ± 9	1.00
		D	205 ± 1	206 ± 0	–	100	66 ± 1 78 ± 2 39 ± 1	0.96
30:70:5	20	A	225 ± 1	214 ± 1	195 ± 3	95	53 ± 1 73 ± 2 33 ± 3	2.92
		B	322 ± 1	297 ± 1	294 ± 2	92	59 ± 1 82 ± 1 29 ± 1	2.07
		C	148 ± 0	147 ± 1	–	100	51 ± 0 62 ± 2 43 ± 4	2.79
		D	247 ± 1	234 ± 1	–	95	56 ± 0 66 ± 2 41 ± 7	2.30
10:90:5	15	A	134 ± 1	120 ± 1	113 ± 1	90	51 ± 1 63 ± 2 29 ± 2	3.83
		B	251 ± 2	239 ± 3	216 ± 1	95	59 ± 1 71 ± 1 32 ± 1	2.97
		C	104 ± 0	99 ± 1	–	95	49 ± 4 58 ± 3 34 ± 4	3.36
		D	185 ± 1	183 ± 1	–	99	50 ± 1 59 ± 2 33 ± 3	2.37

a comparison of the full angular scans before and after protein exposure is shown in Figure 7b–d for each copolymer composition. The sample with 30:70:5 had an unexpectedly high protein adhesion, probably due to defects (e.g., coating delamination during the rather long experiment). However, the data clearly shows that samples 50:50:5 and 10:90:5 are strongly protein-repellent (average protein layer thickness: 2.9 and 0 nm, respectively, see Table 3). This is considerably lower than the fibrinogen adhesion measured for poly(oxanorbornene) SMAMPs, which was around 8 nm.[55] For a second sample set, only the kinetics experiments were performed. These additional data are shown in Table S5 (Supporting Information). They clearly show that the protein repellency of 30:70:5 is on the same order of magnitude as that of 50:50:1, so that the data point of the first series can be considered as an outliner and need not be considered further. Overall, the protein adhesion data shows that the protein adhesion decreases with increasing DMAA content.

2.7. Biological Characterization

The bioactivity of the different **IA-BP-Ester** copolymer coatings is summarized in **Figure 8**. The antimicrobial activity was first evaluated against Gram-negative *Escherichia coli* and Gram-positive *Staphylococcus aureus* bacteria with the so-called spray assay,[65] an assay with a low bacterial load that is used to discriminate between active and inactive coatings (Figure 8a,b). The results are given in % of bacterial growth, which is the percentage of surviving bacteria. The coatings that were active in the spray assay, i.e., those with substantially less than 10% surviving bacteria, were then further analyzed with the Japanese Industrial Standard JIS

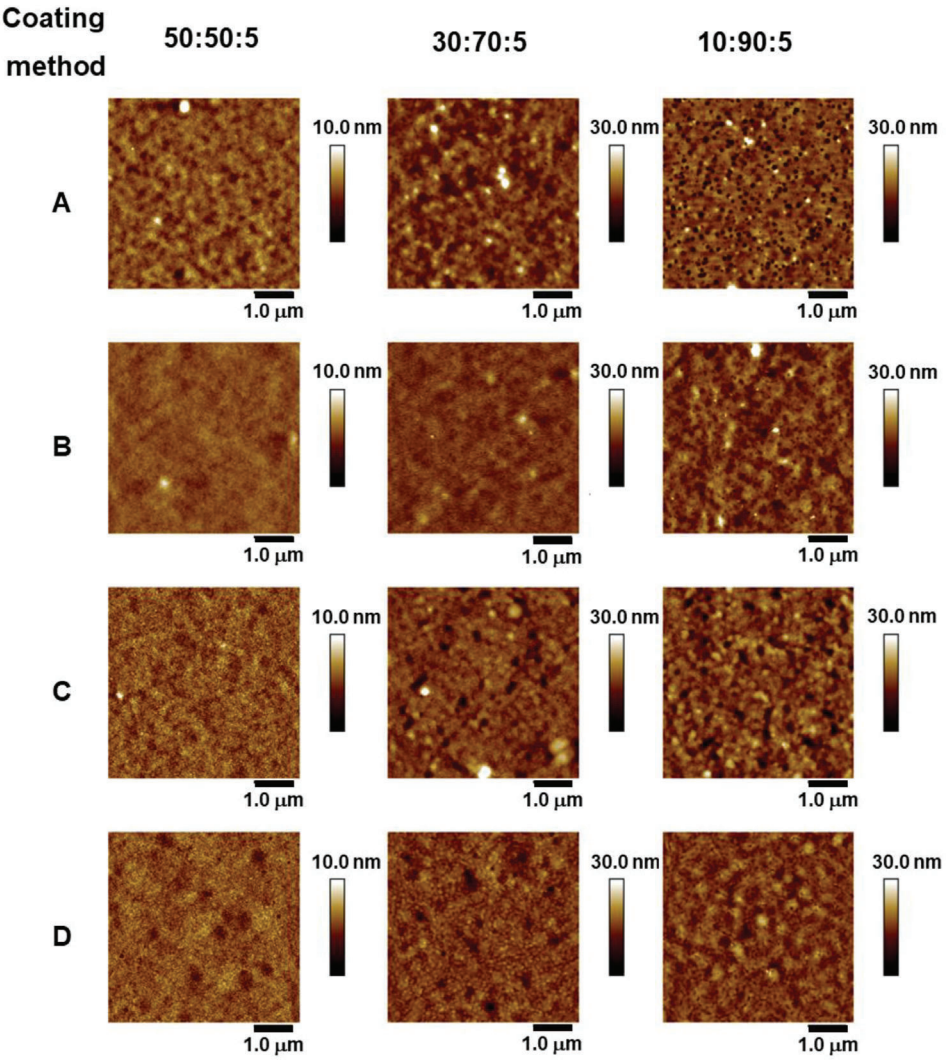

Figure 5. AFM height images of coatings **A**–**D** for the different **IA-BP-Ester** copolymer networks (50:50:5, 30:70:5, 10:90:5).

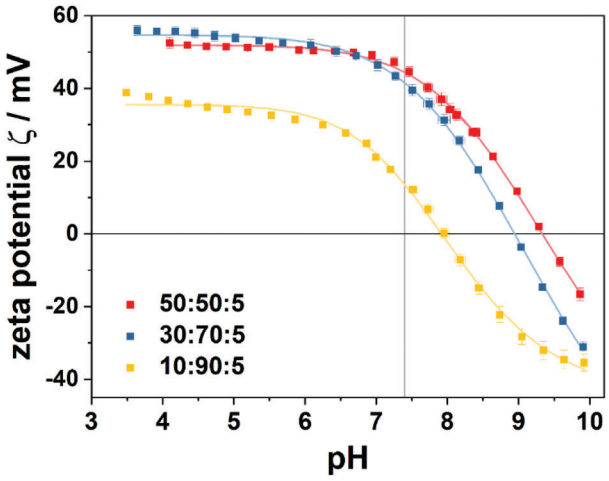

Figure 6. Zeta potential titration curve (ζ vs pH) obtained by electrokinetic measurements for **IA-BP-Ester** coatings (type **B**) with different diitaconate contents (50:50:5, 30:70:5, 10:90:5).

Table 3. Zeta potential titration data and protein adsorption data of **IA-BP-Ester** coatings with different repeat unit ratios. The pK value was estimated as described in the experimental. ζ_{max} = zeta potential in the acidic range, ζ_{phys} = zeta potential at physiological pH.

IA-BP-Ester	Fibrinogen adhesion [nm]	ζ_{max} [mV]	IEP	ζ_{phys} [mV]	pK
50:50:5	2.9	51.9 ± 2	9.3 ± 0.1	44.5 ± 5	8.0 ± 0.2
30:70:5	n.d.	54.7 ± 2	8.9 ± 0.1	41.7 ± 5	8.0 ± 0.2
10:90:5	0	35.5 ± 2	7.9 ± 0.1	13.7 ± 5	7.1 ± 0.2

Z 2801 (JIS-Assay), a standardized assay for antimicrobial polymer surfaces, which uses a much higher bacterial load.[66] The results of the JIS assay are reported as log (reduction), which is the decadic logarithm of the factor by which the bacterial growth on the surface was reduced (i.e., a 3 log reduction corresponds to a growth reduction by 10^3, which is the definition for a substance being bactericidal).

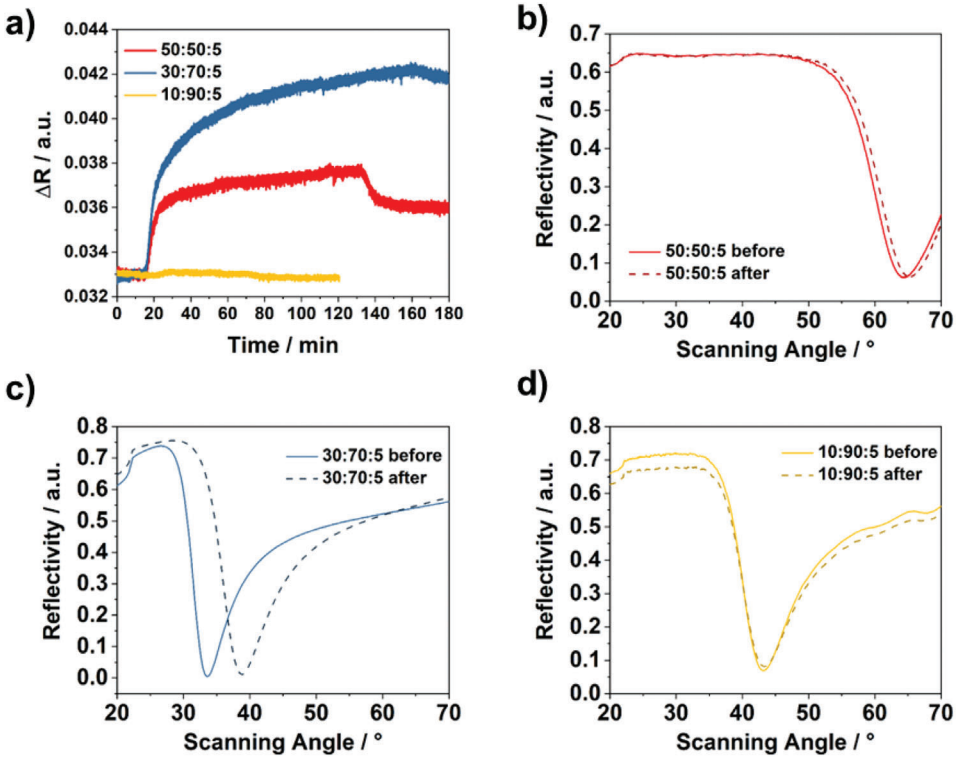

Figure 7. SPR measurements of **IA-BP-Ester** copolymers (type **B**). a) Kinetics experiments for samples 50:50:5, 30:70:5, and 10:90:5. b–d) Full angular reflectivity scans before and after protein exposure for samples 50:50:5, 30:70:5, and 10:90:5.

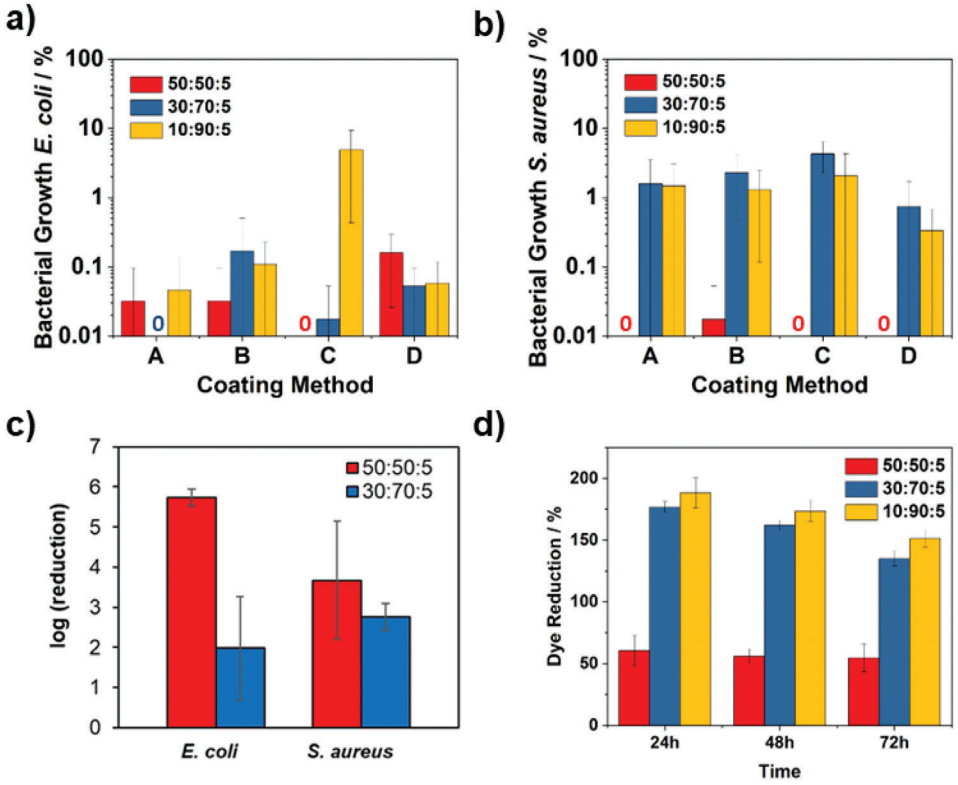

Figure 8. Bioactivity of **IA-BP-Ester** surface coatings. a,b) Bacterial growth of *E. coli* and *S. aureus* on coating types **A**–**D** (in %) in the spray assay; c) bacterial growth (in %) of *E. coli* and *S. aureus* on **B** coatings in the JIS assay; d) metabolic activity (presented as percentage of Alamar Blue dye reduction) of gingiva keratinocytes grown on **B** coatings.

The spray assay data (Figure 8a,b) showed that all three **IA-BP-Ester** copolymer networks were active against *E. coli* bacteria, but that only the polymer with the composition 50:50:5 was sufficiently active against *S. aureus* to kill all bacteria even when challenged with a low bacterial load. The spray assay further revealed that the coating method (**A**–**D**) did not significantly affect the antibacterial activity, and that all coatings were, in principle, sufficiently active to continue to the JIS-Assay. Since the results from the AFM measurements documented that the **B** type coatings were the most homogeneous ones, only these were tested with the JIS assay, where they were challenged with a much higher bacterial load. The **B** type coatings of 10:90:5 were insufficiently active in the JIS assay (data not shown). For the 30:70:5 coatings, a log 2 reduction was found against *E. coli*, while that against *S. aureus* was 2.7. Further, 50:50:5 had a 3.7 log reduction against *E. coli* and a 5.7 log reduction against *S. aureus*, i.e., this polymer coating was bactericidal for both types of bacteria (Figure 8c).

The results of the cell compatibility assay are shown in Figure 8d. Here, the metabolic activity of gingiva keratinocytes grown on **IA-BP-Ester** copolymer networks (type **B**) for 24, 48, and 72 h is presented as dye reduction of the indicator dye Alamar Blue,[67] which is proportional to the metabolic activity of the cells, and thus to their viability. As this assay is only valid to quantitatively assess the cell viability if the same number of cells are compared, the keratinocytes were also imaged by optical microscopy (**Figure 9**a) and the so-called live-dead-stain (an assay in which membrane-damaged cells turn red, while membrane-intact, "living" cells remain green, Figure 9b) to visualize the shape and number of the cell population.

The optical microscopy data (Figure 9a) shows that the cells on the 50:50:5 sample were round, while those on the other two samples and the control were elongated. Thus, they could adhere well to the 30:70:5 and 10:90:5 coatings, but seem to avoid the 50:50:5 coating. The live-dead images further show that cells grown on that substrate aggregated (larger and fewer green spots on the image), as if to avoid contact with the surface by aggregation. In line with these results, it was found that the Alamar Blue dye reduction of cells grown on 50:50:5 was significantly lower than for the other two samples, on which the dye reduction was even higher than the growth control. Since the cells did not attach to 50:50:5, they also could not proliferate and metabolize as affectively as on the other two substrates. Interestingly though, the keratinocytes grown on 50:50:5 were not membrane-compromised.

Overall, the bioactivity data shows that copolymer 50:50:5 had an optimized amount of cationic repeat units, so that a strong antimicrobial activity against *E. coli* and *S. aureus* was observed. At the lower cationic group density of 30:70:5, there was still a marked antimicrobial activity, but apparently the bacterial membranes could not be as efficiently damaged as at the higher diitaconate content. However, sample 30:70:5 showed a significantly better cell compatibility than 50:50:5. Thus, while 50:50:5 would be the material of choice for out-of-patient applications to eradicate bacterial biofilms, 30:70:5 is the better candidate for medical products in direct contact with a patient, e.g., for catheter coatings.

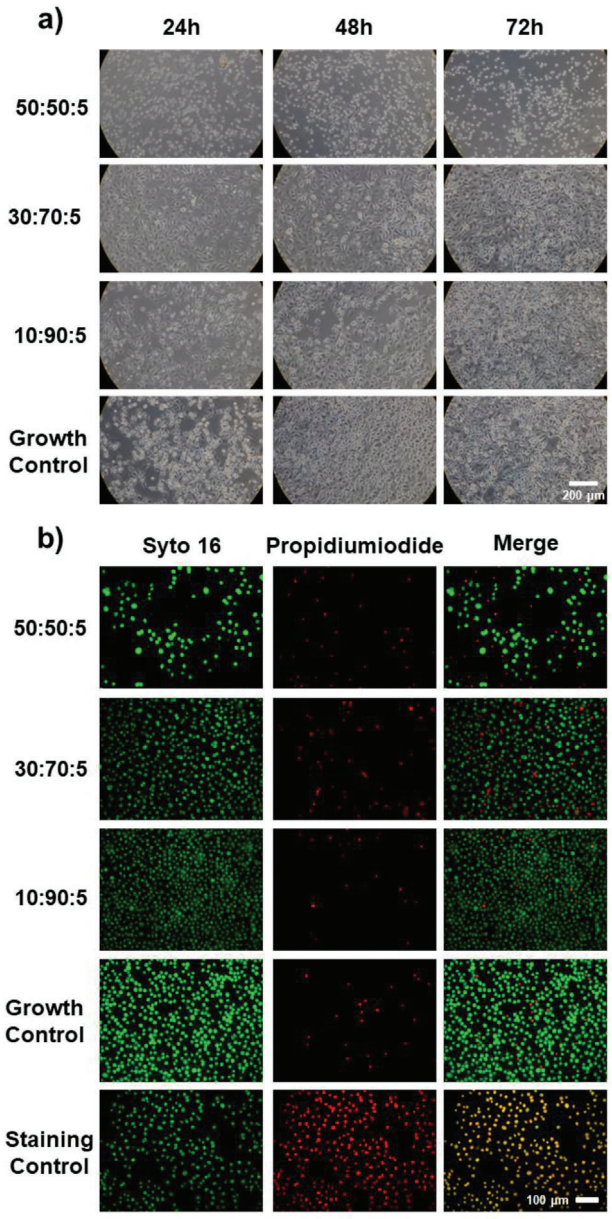

Figure 9. Cell compatibility of **IA-BP-Ester** hydrogels (type **B**). a) Optical micrographs and, b) fluorescence micrographs of cells grown on the coatings. The cell number on the samples 30:70:5 and 10:90:5 was comparable to the growth control, as was the number of membrane compromised (red) cells. The cells on 50:50:5 were more aggregated and round, indicating adhesion problems.

3. Conclusion

In this work, the synthesis and characterization of antimicrobial and protein-repellent polymer coatings consisting of facially amphiphilic, antimicrobial poly(diitaconate) repeat units and protein-repellent dimethylacrylamide repeat units was presented. As surface-attached polymer networks, these coatings are much less prone to attach proteins than previously reported

poly(oxanorbornene)-based cationic surface coatings,[55] and as such are potentially more suitable to prevent biofilm formation. At higher diitaconate content, they had a marked antimicrobial activity against *S. aureus* and *E. coli* bacteria in a range that would make them suitable candidates for medical products. Yet at too high content of the cationic repeat units, the coatings compromise the cell metabolism, which is a sign of beginning cytotoxicity, even though the cells were not membrane-compromised (as indicated by the live–dead assay). It is of additional relevance whether these coatings are sufficiently stable under application conditions, storage conditions, and sterilization conditions to determine their suitability for applications in the biomedical field. This needs to be ascertained in further studies.

4. Experimental Section

All experimental details including the materials synthesis are given in the Supporting Information. Most procedures for the biological characterizaion have been published previously.[65–67]

Supporting Information

Supporting Information is available from the Wiley Online Library or from the author.

Acknowledgements

Gingival mucosal keratinocytes were obtained from human volunteers who had previously given written consent according to the Helsinki declaration. This was approved by the ethics vote number 381/15 of the Ethics Board of the Albert-Ludwigs-Universität, Freiburg, Germany. Funding of this project by the Federal Ministry of Education and Research of Germany (BMBF, ProMat Leben – Polymere, Grant ID 13XP5070A, 13XP5070B "BioSMAMPs") is gratefully acknowledged.

Open access funding enabled and organized by Projekt DEAL.

Conflict of Interest

The authors declare no conflict of interest.

Data Availability Statement

The data that support the findings of this study are available in the Supporting Information of this article.

Keywords

antimicrobial activity, cell compatibility, poly(diitaconate), polycations, protein adhesion

Received: September 9, 2022
Revised: November 8, 2022
Published online: January 29, 2023

[1] F. Siedenbiedel, J. C. Tiller, *Polymers* **2012**, *4*, 46.
[2] A. M. Klibanov, *J. Mater. Chem.* **2007**, *17*, 2479.
[3] E.-R. Kenawy, S. D. Worley, R. Broughton, *Biomacromolecules* **2007**, *8*, 1359.
[4] L. Timofeeva, N. Kleshcheva, *Appl. Microbiol. Biotechnol.* **2011**, *89*, 475.
[5] L. Ferreira, A. Zumbuehl, *J. Mater. Chem.* **2009**, *19*, 7796.
[6] S.-K. Kim, *Chitin, Chitosan, Oligosaccharides and Their Derivatives: Biological Activities and Applications*, CRC Press, Boca Raton **2011**.
[7] E. K. Riga, M. Vöhringer, V. T. Widyaya, K. Lienkamp, *Macromol. Rapid Commun.* **2017**, *38*, 1700216.
[8] P. Zou, W. Hartleb, K. Lienkamp, *J. Mater. Chem.* **2012**, *22*, 19579.
[9] J. C. Tiller, C.-J. Liao, K. Lewis, A. M. Klibanov, *Proc. Natl. Acad. Sci. USA* **2001**, *98*, 5981.
[10] J. C. Tiller, S. B. Lee, K. Lewis, A. M. Klibanov, *Biotechnol. Bioeng.* **2002**, *79*, 465.
[11] J. Lin, J. C. Tiller, S. B. Lee, K. Lewis, A. M. Klibanov, *Biotechnol. Lett.* **2002**, *24*, 801.
[12] J. Lin, S. Qiu, K. Lewis, A. M. Klibanov, *Biotechnol. Bioeng.* **2003**, *83*, 168.
[13] J. Lin, S. Qiu, K. Lewis, A. M. Klibanov, *Biotechnol. Prog.* **2002**, *18*, 1082.
[14] D. Park, J. Wang, A. M. Klibanov, *Biotechnol. Prog.* **2006**, *22*, 584.
[15] N. M. Milović, J. Wang, K. Lewis, A. M. Klibanov, *Biotechnol. Bioeng.* **2005**, *90*, 715.
[16] A. Kanazawa, T. Ikeda, T. Endo, *J. Polym. Sci., Part A: Polym. Chem.* **1993**, *31*, 1467.
[17] E. K. Riga, M. Vöhringer, V. T. Widyaya, K. Lienkamp, *Macromol. Rapid Commun.* **2017**, *38*, 1700216.
[18] L. A. T. W. Asri, M. Crismaru, S. Roest, Y. Chen, O. Ivashenko, P. Rudolf, J. C. Tiller, H. C. Van Der Mei, T. J. A. Loontjens, H. J. Busscher, *Adv. Funct. Mater.* **2014**, *24*, 346.
[19] P. Zou, D. Laird, E. K. Riga, Z. Deng, F. Dorner, H.-R. Perez-Hernandez, D. L. Guevara-Solarte, T. Steinberg, A. Al-Ahmad, K. Lienkamp, *J. Mater. Chem. B* **2015**, *3*, 6224.
[20] K. Lienkamp, A. E. Madkour, A. Musante, C. F. Nelson, K. Nüsslein, G. N. Tew, *J. Am. Chem. Soc.* **2008**, *130*, 9836.
[21] B. P. Mowery, S. E. Lee, D. A. Kissounko, R. F. Epand, R. M. Epand, B. Weisblum, S. S. Stahl, S. H. Gellman, *J. Am. Chem. Soc.* **2007**, *129*, 15474.
[22] B. P. Mowery, A. H. Lindner, B. Weisblum, S. S. Stahl, S. H. Gellman, *J. Am. Chem. Soc.* **2009**, *131*, 9735.
[23] D. Liu, W. F. Degrado, *J. Am. Chem. Soc.* **2001**, *123*, 7553.
[24] K. Kuroda, W. F. Degrado, *J. Am. Chem. Soc.* **2005**, *127*, 4128.
[25] G. N. Tew, R. W. Scott, M. L. Klein, W. F. Degrado, *Acc. Chem. Res.* **2010**, *43*, 30.
[26] E. A. Porter, X. Wang, H.-S. Lee, B. Weisblum, S. H. Gellman, *Nature* **2000**, *404*, 565.
[27] K. Lienkamp, K.-N. Kumar, A. Som, K. Nüsslein, G. N. Tew, *Chemistry* **2009**, *15*, 11710.
[28] K. Lienkamp, A. E. Madkour, K.-N. Kumar, K. Nüsslein, G. N. Tew, *Chemistry* **2009**, *15*, 11715.
[29] K. Lienkamp, G. N. Tew, *Chemistry* **2009**, *15*, 11784.
[30] A. Al-Ahmad, D. Laird, P. Zou, P. Tomakidi, T. Steinberg, K. Lienkamp, *PLoS One* **2013**, *8*, e73812.
[31] G. J. Gabriel, J. G. Pool, A. Som, J. M. Dabkowski, E. B. Coughlin, M. Muthukumar, G. N. Tew, *Langmuir* **2008**, *24*, 12489.
[32] G. J. Gabriel, A. E. Madkour, J. M. Dabkowski, C. F. Nelson, K. Nüsslein, G. N. Tew, *Biomacromolecules* **2008**, *9*, 2980.
[33] I. Ivanov, S. Vemparala, V. Pophristic, K. Kuroda, W. F. Degrado, J. A. Mccammon, M. L. Klein, *J. Am. Chem. Soc.* **2006**, *128*, 1778.
[34] C. W. Avery, E. F. Palermo, A. Mclaughlin, K. Kuroda, Z. Chen, *Anal. Chem.* **2011**, *83*, 1342.
[35] C. W. Avery, A. Som, Y. Xu, G. N. Tew, Z. Chen, *Anal. Chem.* **2009**, *81*, 8365.
[36] K. A. Brogden, *Nat. Rev. Microbiol.* **2005**, *3*, 238.

[37] M. R. Yeaman, N. Y. Yount, *Pharmacol. Rev.* **2003**, *55*, 27.
[38] A. Peschel, R. W. Jack, M. Otto, L. V. Collins, P. Staubitz, G. Nicholson, H. Kalbacher, W. F. Nieuwenhuizen, G. Jung, A. Tarkowski, K. P. M. Van Kessel, J. A. G. Van Strijp, *J. Exp. Med.* **2001**, *193*, 1067.
[39] N. J. Afacan, A. T. Y. Yeung, O. M. Pena, R. E. W. Hancock, *Curr. Pharm. Des.* **2012**, *18*, 807.
[40] K. A. Brogden, M. Ackermann, P. B. Mccray, B. F. Tack, *Int. J. Antimicrob. Agents* **2003**, *22*, 465.
[41] M. Zasloff, *Nature* **2002**, *415*, 389.
[42] I. Sovadinova, E. F. Palermo, M. Urban, P. Mpiga, G. A. Caputo, K. Kuroda, *Polymers* **2011**, *3*, 1512.
[43] A. E. Madkour, A. H. R. Koch, K. Lienkamp, G. N. Tew, *Macromolecules* **2010**, *43*, 4557.
[44] G. J. Gabriel, J. A. Maegerlein, C. F. Nelson, J. M. Dabkowski, T. Eren, K. Nüsslein, G. N. Tew, *Chemistry* **2009**, *15*, 433.
[45] K. Kuroda, G. A. Caputo, W. F. Degrado, *Chemistry* **2009**, *15*, 1123.
[46] E. F. Palermo, K. Kuroda, *Biomacromolecules* **2009**, *10*, 1416.
[47] H. Han, J. Wu, C. W. Avery, M. Mizutani, X. Jiang, M. Kamigaito, Z. Chen, C. Xi, K. Kuroda, *Langmuir* **2011**, *27*, 4010.
[48] Y. Oda, S. Kanaoka, T. Sato, S. Aoshima, K. Kuroda, *Biomacromolecules* **2011**, *12*, 3581.
[49] E. F. Palermo, D. - K. Lee, A. Ramamoorthy, K. Kuroda, *J. Phys. Chem. B* **2011**, *115*, 366.
[50] I. Sovadinova, E. F. Palermo, R. Huang, L. M. Thoma, K. Kuroda, *Biomacromolecules* **2011**, *12*, 260.
[51] M. Mizutani, E. F. Palermo, L. M. Thoma, K. Satoh, M. Kamigaito, K. Kuroda, *Biomacromolecules* **2012**, *13*, 1554.
[52] E. F. Palermo, S. Vemparala, K. Kuroda, *Biomacromolecules* **2012**, *13*, 1632.
[53] K. Kuroda, G. A. Caputo, *Wiley Interdiscip. Rev.: Nanomed. Nanobiotechnol.* **2013**, *5*, 49.
[54] M.-R. Lee, S. S. Stahl, S. H. Gellman, *Org. Lett.* **2008**, *10*, 5317.
[55] M. Kurowska, A. Eickenscheidt, A. Al-Ahmad, K. Lienkamp, *ACS Appl. Bio Mater.* **2018**, *1*, 613.
[56] V. T. Widyaya, C. Müller, A. Al-Ahmad, K. Lienkamp, *Langmuir* **2019**, *35*, 1211.
[57] D. Boschert, A. Schneider-Chaabane, A. Himmelsbach, A. Eickenscheidt, K. Lienkamp, *Chemistry* **2018**, *24*, 8217.
[58] A. Himmelsbach, A. Schneider-Chaabane, K. Lienkamp, *Macromol. Chem. Phys.* **2019**, *220*, 1900346.
[59] C. K. Pandiyarajan, O. Prucker, B. Zieger, J. Rühe, *Macromol. Biosci.* **2013**, *13*, 873.
[60] M. Rendl, A. Bönisch, A. Mader, K. Schuh, O. Prucker, T. Brandstetter, J. Rühe, *Langmuir* **2011**, *27*, 6116.
[61] O. Prucker, C. A. Naumann, J. Rühe, W. Knoll, C. W. Frank, *J. Am. Chem. Soc.* **1999**, *121*, 8766.
[62] O. Prucker, T. Brandstetter, J. Rühe, *Biointerphases* **2017**, *13*, 010801.
[63] A. Himmelsbach, in *Department of Microsystems Engineering*, Albert-Ludwigs-Universität Freiburg, Freiburg **2018**, M.Sc./.
[64] G. Becker, Z. Deng, M. Zober, M. Wagner, K. Lienkamp, F. R. Wurm, *Polym. Chem.* **2018**, *9*, 315.
[65] A. Al-Ahmad, P. Zou, D. L. G. Solarte, E. Hellwig, T. Steinberg, K. Lienkamp, *PLoS One* **2014**, *9*, e111357.
[66] A. Schneider-Chaabane, V. Bleicher, S. Rau, A. Al-Ahmad, K. Lienkamp, *ACS Appl. Mater. Interfaces* **2020**, *12*, 21242.
[67] M. Kurowska, A. Eickenscheidt, D. - L. Guevara-Solarte, V. T. Widyaya, F. Marx, A. Al-Ahmad, K. Lienkamp, *Biomacromolecules* **2017**, *18*, 1373.

